Strain gage radial locations for the accurate determination of mode I stress intensity factors

H. Sarangi[1,*], K.S.R.K. Murthy[2], D. Chakraborty[2*]

[1] Research Scholar, Department of Mechanical Engineering, IIT Guwahati Guwahati 781039, India
[2] Faculty of Department of Mechanical Engineering, Indian Institute of Technology Guwahati, Guwahati 781039, India
* Corresponding author: chakra@iitg.ernet.in

Abstract Strain gage based methods for experimental determination of stress intensity factors (SIFs) are equally powerful as compared to the other methods such as photoelasticity and caustics. However, a major problem with the strain gage methods is the lack of practical recommendations for appropriate radial locations for strain gages for accurate measurement of SIFs. Determination of valid gage locations is thus an open problem. In order to obviate this important problem, a finite element based approach has been suggested in the present investigation for determination of valid or optimal strain gage locations for determination of the mode I SIFs. The proposed approaches are strongly supported by the theory. The present work attempts to estimate the maximum permissible radial distance r_{max} for strain gages (from the crack tip) using the proposed finite element based approaches. This r_{max} of a configuration in turn can be used to obtain the valid locations for strain gages for accurate determination of mode I SIFs. The results of the present investigation show that very accurate values of r_{max} can be obtained using the proposed approach. Dependence of r_{max} on crack length to width ratio has also been investigated in the present work.

Keywords Strain gage, Stress intensity factor, Radial location, Fracture

1. Introduction

The most important parameter in linear elastic fracture mechanics (LEFM) is the stress intensity factor (SIF) as its limiting value decides whether an existing crack in a component grows or not. It is a measure of severity of the crack tip and is frequently used in control of fracture and in life prediction estimations. Accurate values of SIFs are necessary for correct application of LEFM principles in predicting and preventing fracture of the engineering components. Three approaches are currently used to estimate stress intensity factors viz., analytical, numerical and experimental methods. Analytical methods are generally restricted to the simple configurations and collection of such solutions of SIFs can be found in various handbooks [1, 2]. Numerical and experimental techniques are widely used in relatively complex situations [3].

Most widely used experimental techniques for the measurement of SIFs are caustics [4, 5], compliance method [6, 7], photoelasticity [8, 9] and strain gage techniques [10-14]. Among the experimental techniques, strain gage techniques are relatively simple and easy for the determination of SIFs due to direct measurement of strains near the crack tip. Irwin [15] first suggested the use of strain gages for the determination of SIF. However, factors such as the local yielding, high strain gradients, three dimensional state of stress at the crack tips and finite size of the gages strongly affected against the development of strain gage techniques.

To eliminate the above difficulties, Dally and Sanford [10] developed a practically feasible strain gage technique (DS technique) for measuring the static mode I SIF (K_I) in two dimensional

isotropic single ended cracked bodies. A truncated strain series (based on the generalized Westergaard approach [16]) consisting of three unknown coefficients for the representation of the strains has been employed in their technique. A major advantage of their approach is that, only a single strain gage is sufficient to determine mode I SIF and it can be located at a distance sufficiently away from the crack tip. However, no suggestions were made by them on the valid gage locations.

Wei and Zhao [11] proposed a different strain gage method based on the two parameter strain equation which requires two strain gages for measuring the mode I SIF. However, the suggested radial locations of gages necessitate *a priori* knowledge about the plastic zone size which depends on the unknown SIF.

Kuang and Chen [12] employed the asymptotic strain expressions for the measurement of mode I SIF. They suggested that gages could be placed at distances greater than half the thickness of the specimen from the crack tip in spite of the fact that at large distances the measured strains could not be accurately represented by asymptotic equations alone.

It could be seen from the literature that DS technique has been more widely used as compared to other strain gage techniques. While there are some recommendations available for radial locations of strain gage techniques developed by Wei and Zhao [11] and Kuang and Chen [12], no method has been presented until recently for determination of appropriate radial location of strain gages corresponding to the DS technique in experimental determination of the mode I SIFs. Due to uncertainty over the radial location of strain gage in DS technique, very limited amount of work has been published using this technique for corroborating the analytical or numerical SIFs [14]. Determination of valid gage locations for DS technique is thus an open problem.

The present paper aims at development of an efficient finite element based approach for accurate and consistent evaluation of the maximum permissible radial distance $r_{\max}$ for strain gages (from the crack tip) for accurate measurement of mode I SIFs in configurations with single ended cracks. This $r_{\max}$ of a configuration in turn can be used to obtain the valid locations for strain gages for accurate determination of mode I SIFs. Another objective of the present work is to study the dependence of $r_{\max}$ on crack length to width ratio of a given configuration. The proposed numerical methodology is well supported with theory.

2. Theoretical Background

This section describes the background theory for the estimation of $r_{\max}$ value for accurate measurement of mode I SIF using Dally and Sanford [10] single strain gage technique. According to this technique the region around a crack tip is divided into three zones viz. zone I, zone II and zone

III as shown in Fig. 1. Zone I is close to the crack tip and first term of the strain series (singular term) is sufficient to represent the strains within this zone. However, it is not a valid zone for accurate measurement of strains as the stress state in this region is three dimensional [10, 17] and the measured strains will be severely affected by plasticity effects.

Zone III is again not suitable for measurement of strain data because, very large number of terms in the strain series is required to yield accurate results. Therefore, the intermediate region or zone II is favorable and optimum zone for accurate measurement of the surface strains. This is defined as a zone in which a singular term and a small number of higher order terms will accurately describe the strain field.

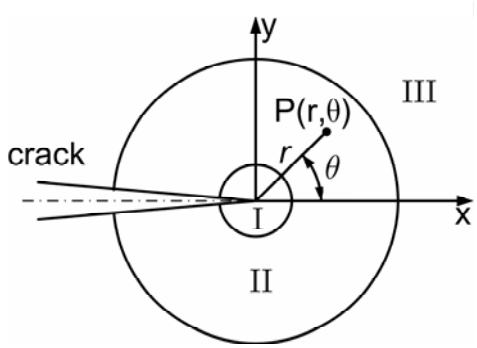

Figure 1. Different zones at the crack tip

The generalized Westergaard approach can be employed to obtain the expressions of different strain components within the zone II. The modified Airy stress function in this approach is given by [16]

$$\phi = \mathrm{Re}\,\overline{\overline{Z}}(z) + y\,\mathrm{Im}\,\overline{Z}(z) + y\,\mathrm{Im}\,\overline{Y}(z) \tag{1}$$

where

$$\frac{d\overline{\overline{Z}}}{dz} = \overline{Z}, \quad \frac{d\overline{Z}}{dz} = Z, \text{ and } \quad \frac{d\overline{Y}}{dz} = Y \tag{2}$$

and the complex analytic functions $Z(z)$ and $Y(z)$ are defined as

$$Z(z) = \sum_{n=0}^{\infty} A_n\, z^{n-\frac{1}{2}} = \frac{K}{\sqrt{2\pi z}} + \sum_{n=1}^{\infty} A_n\, z^{n-\frac{1}{2}} \tag{3}$$

$$Y(z) = \sum_{m=0}^{\infty} B_m\, z^m = \frac{\sigma_{0x}}{2} + \sum_{m=1}^{\infty} B_m\, z^m \tag{4}$$

which are series type functions (in terms of complex variable $z = x + iy$) containing infinite number of coefficients ($A_1, A_2, ..., A_\infty$; $B_1, B_2, ..., B_\infty$). The strain field in the zone II can be sufficiently represented by the three parameter series with unknown coefficients A_0, A_1 and B_0 [10] which depend on boundary conditions. Assuming plane stress conditions, the three term representation of strain field in this zone is therefore,

$$
\begin{aligned}
2G\,\varepsilon_{xx} &= A_0\, r^{-1/2}\cos\frac{\theta}{2}\left[\kappa-\sin\frac{\theta}{2}\sin\frac{3\theta}{2}\right]+\frac{2B_0}{(1+\nu)}+A_1\, r^{1/2}\cos\frac{\theta}{2}\left[\kappa+\sin^2\frac{\theta}{2}\right]\\
2G\varepsilon_{yy} &= A_0\, r^{-1/2}\cos\frac{\theta}{2}\left[\kappa+\sin\frac{\theta}{2}\sin\frac{3\theta}{2}\right]-\frac{2\nu B_0}{(1+\nu)}+A_1\, r^{1/2}\cos\frac{\theta}{2}\left[\kappa-\sin^2\frac{\theta}{2}\right]\\
2G\,\gamma_{xy} &= A_0\, r^{-1/2}\left[\sin\theta\cos\frac{3\theta}{2}\right]-A_1\, r^{1/2}\left[\sin\theta\cos\frac{\theta}{2}\right]
\end{aligned}
\tag{5}
$$

where $\kappa=(1-\nu)/(1+\nu)$ and A_0, A_1 and B_0 are unknown coefficients which can be determined using geometry of the specimen and loading conditions. Using the definition of K_I it can be shown that

$$K_I=\sqrt{2\pi}\,A_0 \tag{6}$$

The strain component ε_{aa} at the point *P* located by r and θ (Fig. 2) is given by

$$
\begin{aligned}
2G\varepsilon_{aa} &= A_0\, r^{-1/2}\left[\kappa\cos\frac{\theta}{2}-\frac{1}{2}\sin\theta\sin\frac{3\theta}{2}\cos 2\alpha+\frac{1}{2}\sin\theta\cos\frac{3\theta}{2}\sin 2\alpha\right]\\
&+A_1\, r^{1/2}\cos\frac{\theta}{2}\left[\kappa+\sin^2\frac{\theta}{2}\cos 2\alpha-\frac{1}{2}\sin\theta\sin 2\alpha\right]+B_0\left(\kappa+\cos 2\alpha\right)
\end{aligned}
\tag{7}
$$

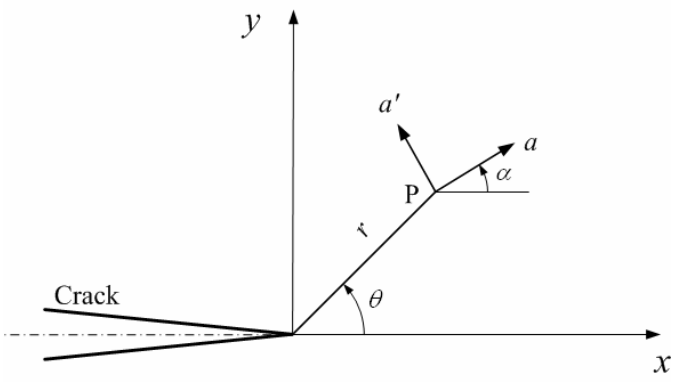

Figure 2. Strain gage orientation and location

The coefficient of B_0 term in Eq. (7) can be eliminated by selecting the angle α such that

$$\cos 2\alpha=-\kappa \quad =-\frac{1-\nu}{1+\nu} \tag{8}$$

Similarly coefficient of A_1 can also be made zero if the angle θ is selected as

$$\tan\frac{\theta}{2}=-\cot 2\alpha \tag{9}$$

Thus by placing a single strain gage (Fig. 2) with α and θ as defined by Eqs. (8) and (9) the

strain ε_{aa} can be measured which in turn is related to K_I by

$$2G\varepsilon_{aa} = \frac{K_{\mathrm{I}}}{\sqrt{2\pi r}}\left[\kappa\cos\frac{\theta}{2} - \frac{1}{2}\sin\theta\sin\frac{3\theta}{2}\cos 2\alpha + \frac{1}{2}\sin\theta\cos\frac{3\theta}{2}\sin 2\alpha\right] \tag{10}$$

It should be noted that the above equation accurately determines ε_{aa} upto a radial distance say $r_{\max}$ and it can be written as

$$\varepsilon_{aa} = \frac{1}{\sqrt{r}}\left[\frac{K_{\mathrm{I}}}{G\sqrt{8\pi}}\left(\kappa\cos\frac{\theta}{2} - \frac{1}{2}\sin\theta\sin\frac{3\theta}{2}\cos 2\alpha + \frac{1}{2}\sin\theta\cos\frac{3\theta}{2}\sin 2\alpha\right)\right] \tag{11}$$

For a given configuration, applied load, Young's modulus E and Poisson's ratio ν the expression within the square bracket on the right hand side of Eq. (11) is a constant. Therefore,

$$\varepsilon_{aa} = \frac{C}{\sqrt{r}} \tag{12}$$

where C is a constant. Taking logarithm on both sides of Eq. (12)

$$\ln(\varepsilon_{aa}) = -\frac{1}{2}\ln(r) + \ln(C) \tag{13}$$

Eq. (13) is valid along the line given by Eq. (9) for $r \le r_{\max}$. Thus a plot of Eq. (12) on log-log axes depicts a straight line of slope equals to – 0.5, with an intercept of $\ln(C)$. Theoretically, the straight line property will break beyond $r > r_{\max}$ as more than three parameters are needed in Eq. (7) to estimate the ε_{aa}. Using the straight line property exhibited by Eq. (13), the value of $r_{\max}$ can be accurately estimated from the log-log plots of ε_{aa} and r.

Several experimental and numerical studies have established that 3D effects prevailed up to a radial distance equal to half the thickness of the plate from the crack tip [17]. It was reported that the state of stress is neither plane stress or plane strain within this distance [10, 17]. Therefore, the minimum radial distance $r_{\min}$ for strain measurements on the free surface should be grater than half the thickness of the plate. As a consequence, the optimal or valid radial location r for strain gage in DS technique can now be given as

$$r_{\min}\left(=\frac{1}{2}\text{thickness of plate}\right) \le r \le r_{\max} \tag{14}$$

3. Results and Discussion

In this section, $r_{\max}$ is determined for a single-ended cracked plate using the theoretical formulation described in Section 2. For this purpose, edge cracked plates (Fig. 3(a)) with $a/b=0.1-0.8$ (in steps 0.1) and subjected to uniform tensile stress are considered in this study. Due to symmetry only half of the domain as shown in Fig. 3(b) is employed for FEA. Width $b=1200\,\text{mm}$ and $h/b=3.0$ are considered for this example. Poisson's ratio $\nu=1/3$, and Young's modulus $E=200\,\text{GPa}$ have been assumed. The applied stress σ is set to 100 MPa. Plane stress conditions have been assumed.

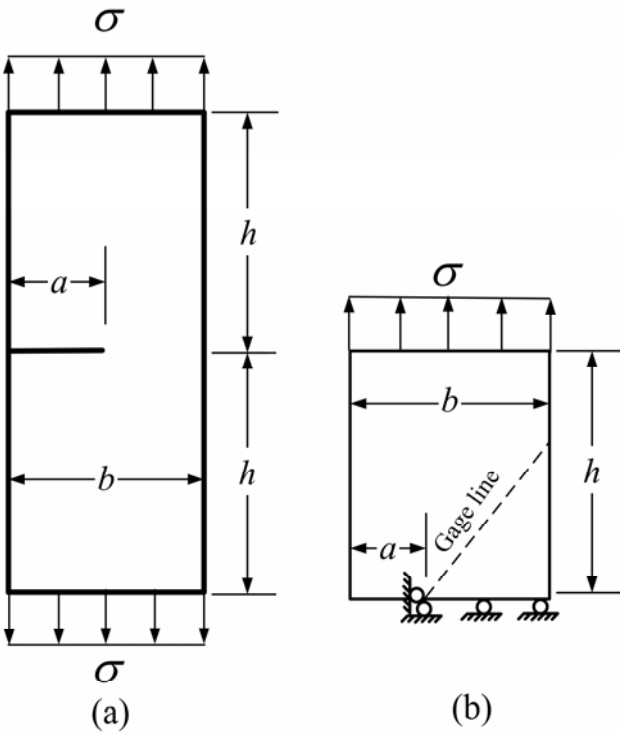

Figure 3. (a) A typical edge cracked plate (b) solution domain for edge cracked plate

To determine the $r_{\max}$ value of the above configurations, a typical finite element mesh for one half of the plate is shown in Fig. 4 (a). The mesh (Fig. 4(a)) is so designed that nodes of several elements are made to lie along the gage line which makes an angle of θ with the axis of crack (Eq. 9). In all the meshes, this line (gage line) begins at the crack tip and terminates at the outer boundaries of the cracked plate. According to DS technique, a single strain gage is required to be placed at an appropriate location on the gage line in the direction of α (Eq. 8) in order to measure the linear strain ε_{aa}. The strains calculated in global coordinate along the gage line are then transformed into linear strain ε_{aa} in the direction α. The radial distances (r) of each of the nodes on the gage line from the crack tip are then computed.

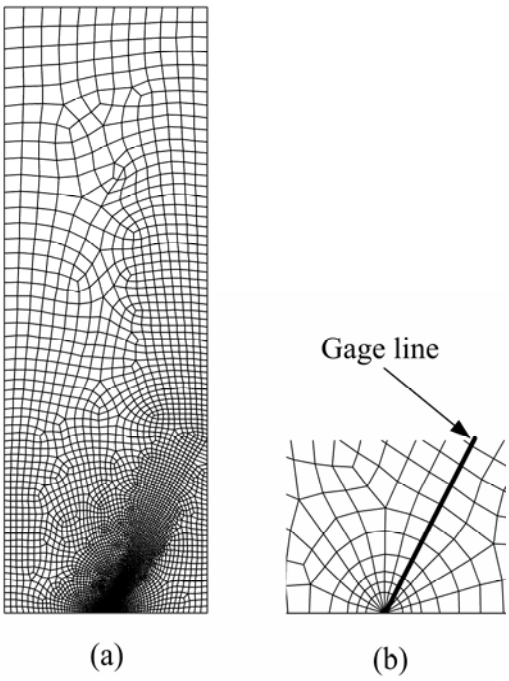

Figure 4. (a) Typical mesh used for edge cracked plate (b) enlarged view at the crack tip corresponding mesh

Following the procedure described in section 2, plot of $\ln(\varepsilon_{aa})$ versus $\ln(r)$ for all values of a/b is shown in Fig. 5. Crack tip point is not plotted as the radius of this point is zero. It is interesting to notice from Fig. 5 that, each plot consists of distinguishable linear portion followed by nonlinear portion (in logarithmic scale) as predicted by theory (section 2). The linear trend distinctly exists up to a certain radial distance and thereafter gradually turns to the nonlinear portion. This can be observed in plots for all values of a/b of edge cracked plate.

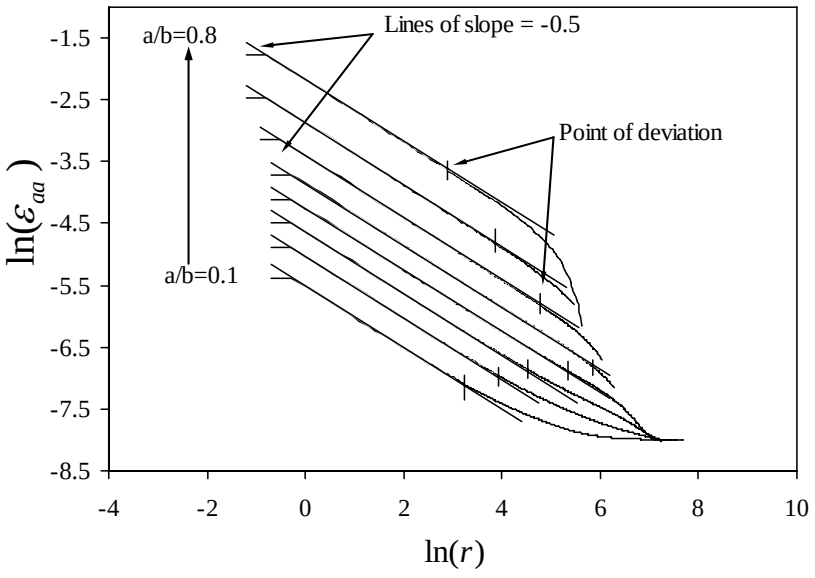

Figure 5. Variation of $\ln(\varepsilon_{aa})$ with $\ln(r)$ along the gage line for the edge cracked plates

As discussed earlier, the initial linear part is due to the dominance of the three parameters and nonlinear part is due to the presence of more than three parameters in the expression in equation for ε_{aa} (Eq. 7). The end point of the linear portion of the plots in Fig. 5 clearly indicates the extent of the three parameter strain series which is the upper bound for strain gage locations i.e. $r_{\max}$ according to the proposed theory.

For determination of $r_{\max}$, straight lines having slope of -0.5 are superposed onto the all plots of $\ln(\varepsilon_{aa})$ versus $\ln(r)$ in Fig. 5. It is interesting to notice from Fig. 5 that both the initial straight line portion of the plots and superposed lines are congruent to each other up to a certain radial distance for all a/b values and the numerical results deviate from the superposed line thereafter due to the dominance of coefficients other than A_0, A_1 and B_0 in Eq. (7). The estimated values of maximum permissible radial distance $r_{\max}$ or the extent of validity of the three parameter zone are marked in Fig. 5 as per the procedure described in [18]. The corresponding numerical values of the $r_{\max}$ are presented in Table 1. A plot of variation of $r_{\max}$ with a/b is also presented in Fig. 6.

It can be seen from the results of Table 1 and Fig. 6 that as the crack length is increased, the value of $r_{\max}$ increases initially until it reaches a maximum value around $a/b = 0.5$ ($r_{\max}$ = 505.34 mm) and thereafter it decreases with the increase of the crack length.

Table 1 Variation of the $r_{\max}$ with crack length a/b

a/b	a (mm)	$r_{\max}/b$
0.1	120	0.021
0.2	240	0.043
0.3	360	0.077
0.4	480	0.174
0.5	600	0.290
0.6	720	0.101
0.7	840	0.040
0.8	960	0.015

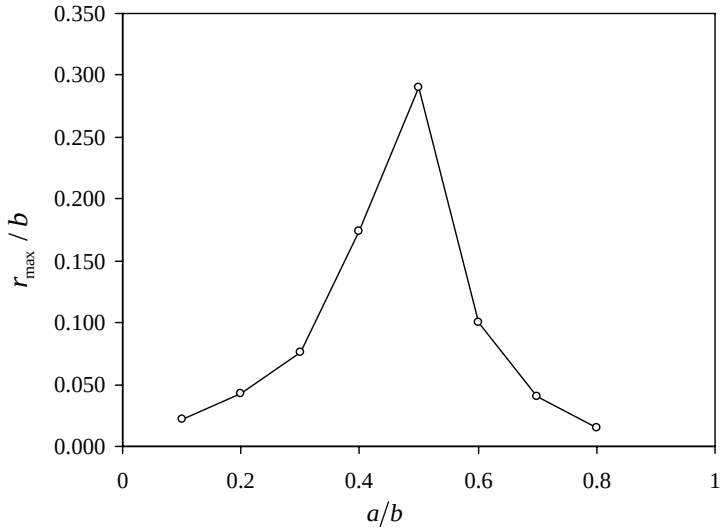

Figure 6. Graph of the r_{max} as a function of a/b (0.1-0.8) for the edge cracked plate.

4. Conclusions

In this paper, a finite element based approach is presented for determination of the valid or optimal radial location of strain gages corresponding to DS technique. The proposed approach is based on efficient computation of the maximum permissible radial distance r_{max} of a strain gage. The existence and determination of the r_{max} is shown theoretically. To demonstrate the proposed approach single ended cracked configurations have been analyzed. Variation of the computed strains in the direction of strain gage along the gage line is as per the theoretical predictions. The results of present investigation show that the maximum permissible radial distance (r_{max}) increases initially with the increase in a/b and decreases with further increase in a/b values. The present method will be extremely useful in placing strain gages for accurate experimental determination of the SIF using DS technique.

Acknowledgements

Authors gratefully acknowledge financial support from the Naval Research Board (NRB), Ministry of Defence, India, under grant number NRB-167/MAT/08-09.

References

[1] H. Tada, P.C. Paris, G.R. Irwin, The stress analysis of cracks handbook. ASME, New York, 2000.

[2] Y. Murakami, Stress intensity factors handbook, Pergamon, England, 1987.

[3] R.J. Sanford, Principles of fracture mechanics, Prentice Hall, NJ, 2003.

[4] K. Konsta-Gdoutos, Limitations in mixed-mode stress intensity factor evaluation by the method of caustics. Eng Fract Mech, 55 (1996) 371–382.

[5] P.S. Theocaris, Local yielding around a crack tip in Plexiglas. J Appl Mech, 37 (1970) 409–415.

[6] R.M. Bonesteel, D.E. Pipers, A.T. Davinroy, Compliance and calibration of double cantilever beam (DCB) specimens. Eng Fract Mech, 10 (1978) 425–428.

[7] J.C. Jr Newman, Stress-intensity factors and crack-opening displacements for round compact specimens. Int J Fract, 17 (1981) 567–578.

[8] E.E. Gdoutos, P.S. Theocaris, A photoelastic determination of mixed-mode stress intensity factors. Exp Mech, 18 (1978) 87–96.

[9] T.H. Hyde, N.A. Warrior, An improved method for determination of photoelastic stress intensity factors using the Westergaard stress function. Int J Mech Sci, 32 (1990) 265–273.

[10] J.W. Dally, R.J. Sanford, Strain gage methods for measuring the opening mode stress intensity factor. Exp Mech, 27 (1987) 381–388.

[11] J. Wei, J.H. Zhao, A two-strain-gage technique for determining mode I stress-intensity factor. Theor Appl Fract Mech, 28 (1997) 135–140.

[12] J.H. Kuang, L.S. Chen, A single strain gage method for measurement. Eng Fract Mech, 51 (1995) 871–878.

[13] J.R. Berger, J.W. Dally, An overdeterministic approach for measuring using strain gages. Exp Mech, 28 (1988) 142–145.

[14] S. Swamy, M.V. Srikanth, K.S.R.K. Murthy, P.S. Robi, Determination of the mode I stress intensity factors of the complex configurations using the strain gages. J Mech Mater Struct, 3 (2008) 1239–1255.

[15] G.. R. Irwin, Analysis of stresses and strains near the end of a crack traversing a plate. J Appl Mech, 24 (1957) 361- 364.

[16] R.J. Sanford, A critical re-examination of the Westergaard method for solving opening-mode crack problems. Mech Res Comm, 6 (1979) 289–294.

[17] J. Rosakis, K. Ravi-Chandar, On crack-tip stress state: An experimental evaluation of three-dimensional effects. Int J Solids Struct, 22 (1986) 121–134.

[18] H. Sarangi, K.S.R.K. Murthy, D. Chakraborty, Optimum Strain gage location for evaluating stress intensity factors in single and double ended cracked Configurations. Eng Fract Mech, 77 (2010) 3190-3203.